ISSN 1027-4510, Journal of Surface Investigation: X-ray, Synchrotron and Neutron Techniques, 2025, Vol. 19, No. 1, pp. 106–114. © Pleiades Publishing, Ltd., 2025.

On the Wave Functions of Positrons Channeling along the [111] Direction in a Silicon Crystal

V. V. Syshchenko[a], *, A. I. Tarnovsky[a], A. S. Parakhin[a], and A. Yu. Isupov[b]

[a] *Belgorod State University, Belgorod, 308015 Russia*

[b] *Laboratory of High Energy Physics, Joint Institute for Nuclear Research, Dubna, 141980 Russia*

**e-mail: syshch@yandex.ru*

Received June 29, 2024; revised August 25, 2024; accepted August 25, 2024

Abstract—For a positively charged particle, the repulsive continuous potentials of three adjacent [111] string in a silicon crystal create a shallow potential well with the symmetry of an equilateral triangle, which is described by the C_{3v} group. The quantum motion of a particle in such a well is of interest in the context of quantum chaos phenomena. A previously developed numerical procedure for determining energy levels and wave functions of stationary states, which takes into account the symmetry of this problem, is applied to investigate the transverse motion of channeled positrons with energies of 5, 6, and 20 GeV. A classification of stationary states in transverse motion is proposed based on the theory of group representations. The wave functions of stationary states in an axially symmetric potential well are also determined, and the modification of these functions under the influence of a perturbation with equilateral triangle symmetry is demonstrated. In the upper region of the triangular potential well, classical motion is chaotic for the vast majority of initial conditions. The structure of the obtained wave functions in this region exhibits characteristic features predicted by the theory of quantum chaos.

Keywords: channeling, silicon, numerical simulation, spectral method, hexagonal grid, triangular symmetry, quantum chaos

DOI: 10.1134/S102745102570017X

INTRODUCTION

A fast charged particle moving through a crystal at a small angle relative to the direction of a densely packed atomic string can become confined within a potential well formed by one or a number of such strings, undergoing finite motion in the transverse plane, which is a phenomenon known as axial channeling [1–4]. In this case, the particle's motion can be accurately described using the continuous potential approximation, where the atomic-string potential is averaged along its axis [5]. Within this potential field, the longitudinal component of the particle's momentum $p_{\|}$ is conserved, which reduces the problem of particle motion to a two-dimensional problem in the transverse plane.

It is well established (e.g., [1]) that quantum effects can manifest during the channeling of fast particles in crystals. A series of previous studies [6–10] investigated these effects in the case of electron channeling along the [110] direction of a silicon crystal, while in [11–14], the developed approach was extended to the channeling of both electrons and positrons along the [100] direction of a silicon crystal. The latter case is particularly interesting because the phase space of channeled particles contains regions of both regular and chaotic dynamics. The symmetry of the potential in which transverse motion occurs in these two cases corresponds to the C_{2v} and C_{4v} symmetry groups, representing rectangular and square symmetry, respectively [15]. These studies confirmed the predictions of quantum chaos theory [16–19] regarding both the statistical properties of energy-level distributions and the nature of individual quantum states when the motion of a channeled particle exhibits chaotic behavior in the classical limit. Of particular interest, however, is the case of particle motion in a potential field with equilateral triangular symmetry, which corresponds to the C_{3v} symmetry group. We note that this symmetry characterizes the Hénon–Heiles model potential, which was examined in one of the pioneering studies on dynamical chaos [20]. Furthermore, one of the seminal investigations of chaos-assisted tunneling [21] was also conducted for a potential exhibiting triangular symmetry.

In the present study, the numerical method from [22] is used to determine the energy level sets of transverse motion and the corresponding wave functions of stationary states for positrons channeled along the [111] direction of a silicon crystal. In this case, the repulsive potentials of neighboring atomic strings cre-

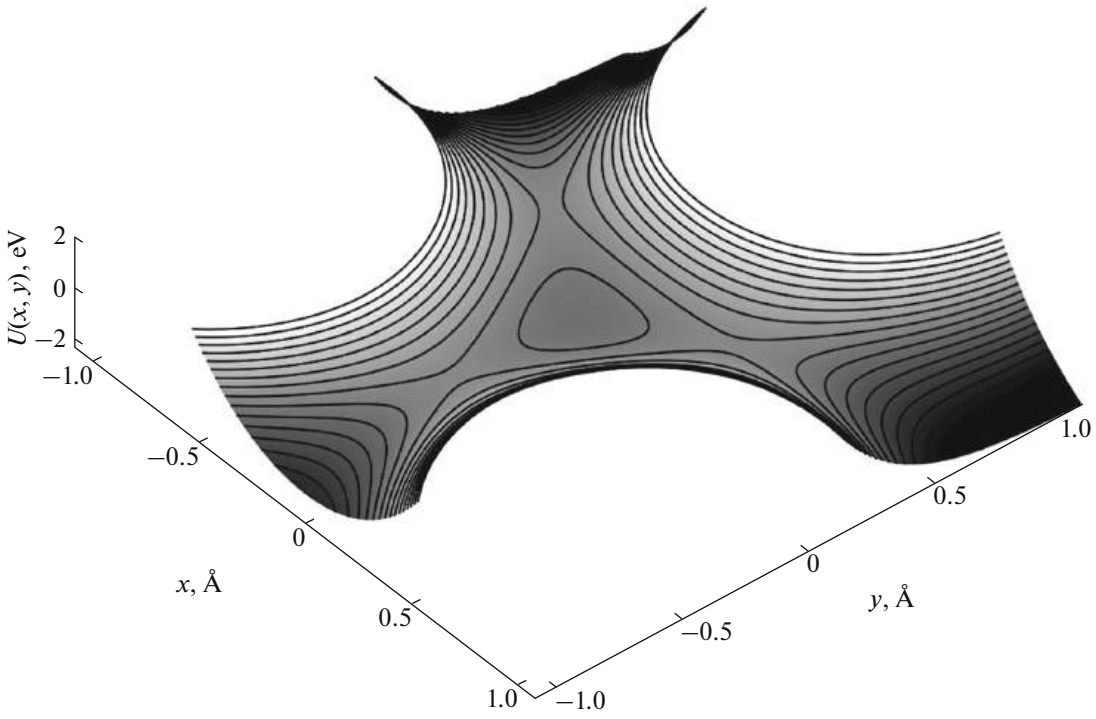

Fig. 1. Potential energy (1) of a positron moving near the [111] direction of a silicon crystal.

ate a shallow potential well exhibiting C_{3v} symmetry. The study discusses the qualitative characteristics of the obtained wave functions and classifies them according to irreducible representations of the C_{3v} group. Additionally, the relationship between these wave functions and those of a particle in a two-dimensional axially symmetric potential well is examined. The parameters of the latter are chosen to ensure the same average semiclassical energy level density as that of the considered well in a silicon crystal.

SIMULATION PROCEDURE

The motion of a relativistic particle in a crystal at a small angle to a densely packed crystallographic axis can be described as two-dimensional motion in the transverse plane (relative to this axis) under the influence of continuous potentials averaged along the atomic strings normal to this plane while conserving the longitudinal component of the particle's momentum $p_{\|}$. In the (111) plane of a silicon crystal, such atomic strings form a hexagonal lattice with a primitive cell side length given by $a = a_z/\sqrt{6} \approx 2.217$ Å, where a_z is the lattice period of silicon. For a positron, the continuous potential of an atomic string is repulsive, and a shallow potential well forms near the center of a triangle whose vertices correspond to the three nearest atomic strings (Fig. 1). Within this well, a positron can undergo finite motion in the transverse plane, a phenomenon known as axial channeling. The positron's potential energy, taking into account the contributions of these three atomic strings, is described by the following sum:

$$U(x,y) = U_1\left(x, y - \frac{a}{\sqrt{3}}\right) + U_1\left(x + \frac{a}{2}, y + \frac{a}{2\sqrt{3}}\right) + U_1\left(x - \frac{a}{2}, y + \frac{a}{2\sqrt{3}}\right) - 7.8571\,\text{eV}, \quad (1)$$

where the constant is selected such that the potential is zero at the center of the triangle. The continuous potential of a single atomic string is approximated by the following equation [1]:

$$U_1(x,y) = U_0 \ln\left(1 + \frac{\beta R^2}{x^2 + y^2 + \alpha R^2}\right), \quad (2)$$

where for the [111] string of the silicon crystal, $U_0 =$ 58.8 eV, $\alpha = 0.37$, $\beta = 2.0$, and $R = 0.194$ Å (Thomas–Fermi radius). The transverse motion states of the positron are described by the Hamiltonian

$$\hat{H} = -\frac{c^2\hbar^2}{2E_{\|}}\left(\frac{\partial^2}{\partial x^2} + \frac{\partial^2}{\partial y^2}\right) + U(x,y), \quad (3)$$

in which the quantity $E_{\|}/c^2$ plays the role of the particle's mass, and $E_{\|} = (m^2c^4 + p_{\|}^2c^2)^{1/2}$ is the energy of longitudinal motion [1].

The determination of eigenfunctions and eigenvalues of the Hamiltonian (3) with potential (1) is only possible numerically. The approach presented is based on the so-called spectral method for finding the eigen-

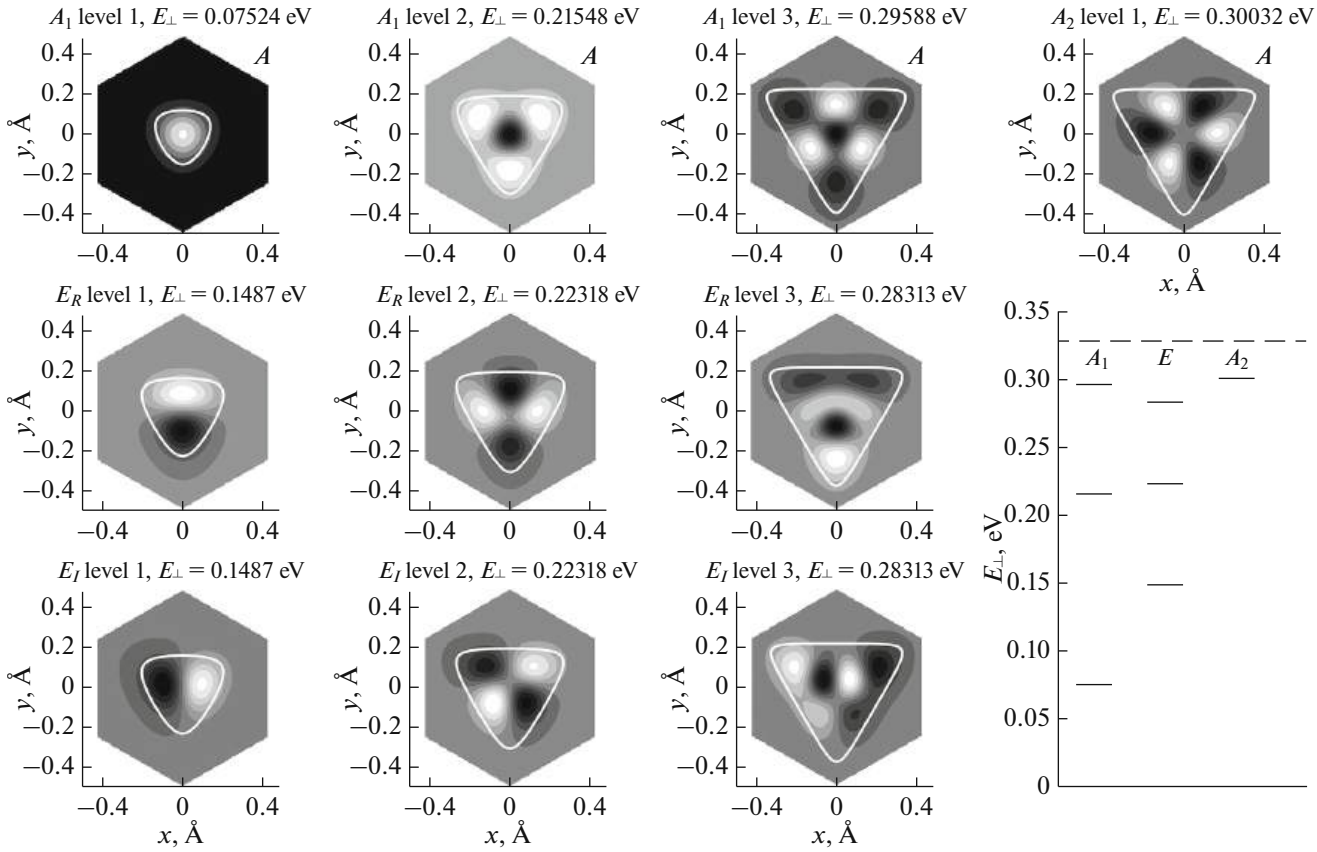

Fig. 2. Graphs of the eigenfunctions of the discrete spectrum of the transverse motion of positrons with the energy $E_\parallel = 6$ GeV in a potential well (1), with lines marking the classical boundaries of motion $U(x, y) = E_\perp$. The energy levels of the transverse motion of positrons are also shown, with a horizontal dashed line marking the height of the saddle point of the potential (1) $U = 0.3278$ eV.

values and eigenfunctions of the Hamiltonian [23] (the details of which, as concerns the channeling problem, are described in [6–9, 24, 25]). This method involves numerical simulation of the time evolution of a wave packet, which is described by the time-dependent Schrödinger equation. A specific feature of the numerical solution of the quantum-mechanical problem with potential (1) is the need to define the wave function on a hexagonal discrete grid. It was shown in [22] that using a square grid leads to the emergence of nonphysical artifacts. A procedure that takes into account the symmetry of the problem, which uses a hexagonal grid, was described there, and the absence of artifacts was demonstrated. This procedure is employed in the present work.

To investigate the spectrum of the Hamiltonian (3), its eigenstates must be classified according to the symmetry properties of potential (1). Since potential (1) exhibits the symmetry of an equilateral triangle, all available transverse motion states can be classified according to irreducible representations of the C_{3v} group (or its isomorphic group D_3) [15], based on the type of symmetry of the wave function. The group elements include the identity transformation I, rotations about angles of $2\pi/3$ and $4\pi/3$, denoted R and R^2, reflection in the "vertical" plane P, and the combinations PR and PR^2. This group has two one-dimensional irreducible representations, denoted A_1 and A_2, which correspond to nondegenerate energy levels, and one two-dimensional representation, denoted E, which corresponds to doubly degenerate energy levels. The function that remains invariant under all transformations forms the basis for the one-dimensional irreducible representation A_1. An initial wave packet that satisfies this requirement can be easily constructed from the results of applying all the group operators to a nonsymmetric Gaussian wave packet ψ_0, with the operators being summed with equal weights:

$$\psi^{(A_1)} = \psi_0 + R\psi_0 + R^2\psi_0 + P\psi_0 + PR\psi_0 + PR^2\psi_0. \quad (4)$$

The function that changes sign upon reflection,

$$\psi^{(A_2)} = \psi_0 + R\psi_0 + R^2\psi_0 - P\psi_0 - PR\psi_0 - PR^2\psi_0, \quad (5)$$

forms the basis for the representation A_2.

Since the complete set of eigenfunctions of a real Hamiltonian can always be selected to be real (e.g., [19]), it is convenient to select two linearly indepen-

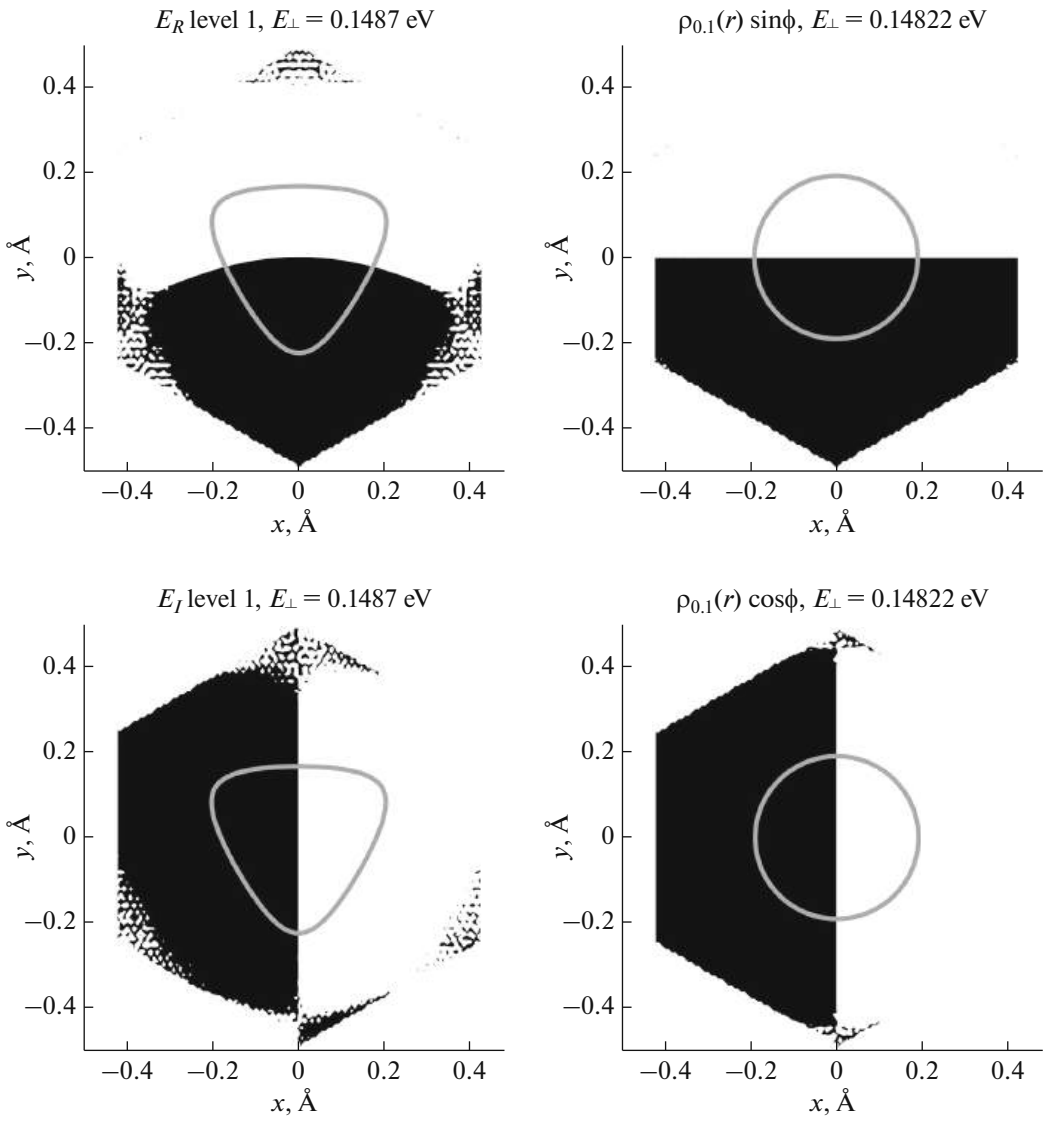

Fig. 3. Comparison of the wave functions of states with $E_\perp = 0.1487$ eV in a potential well (1) and wave functions of states with $E_\perp = 0.14822$ eV in a potential well (8), with lines marking the classical boundaries of motion $U(x, y) = E_\perp$. The irregularity of the black and white regions far from the center of the potential well is due to uncertainties in numerical simulation.

dent wave packets containing only doubly degenerate states as linear combinations of the form

$$\psi^{(E_R)} = \psi_0 - \frac{1}{2}R\psi_0 - \frac{1}{2}R^2\psi_0 + P\psi_0 - \frac{1}{2}PR\psi_0 - \frac{1}{2}PR^2\psi_0, \quad (6)$$

$$\psi^{(E_I)} = \frac{\sqrt{3}}{2}R\psi_0 - \frac{\sqrt{3}}{2}R^2\psi_0 - \frac{\sqrt{3}}{2}PR\psi_0 + \frac{\sqrt{3}}{2}PR^2\psi_0. \quad (7)$$

The first of these functions remains invariant upon reflection P, while the second changes sign. Under rotation operations, the graphs of these functions rotate by the corresponding angle. At first glance, this behavior corresponds to a reducible representation of the group; however, from functions (6) and (7), one can construct a basis for the two-dimensional irreducible representation E by considering them as the real and imaginary parts of complex basis functions. Indeed, the functions

$$\psi_1^{(E)} = \psi^{(E_R)} + i\psi^{(E_I)}, \quad \psi_2^{(E)} = \psi^{(E_R)} - i\psi^{(E_I)}$$

transform into each other under reflections, and acquire a phase factor under rotations.

RESULTS AND DISCUSSION

In the study, the wave functions of stationary states of transverse motion in a potential well (1) for positrons with energies $E_\parallel = 5$, 6, and 20 GeV were calcu-

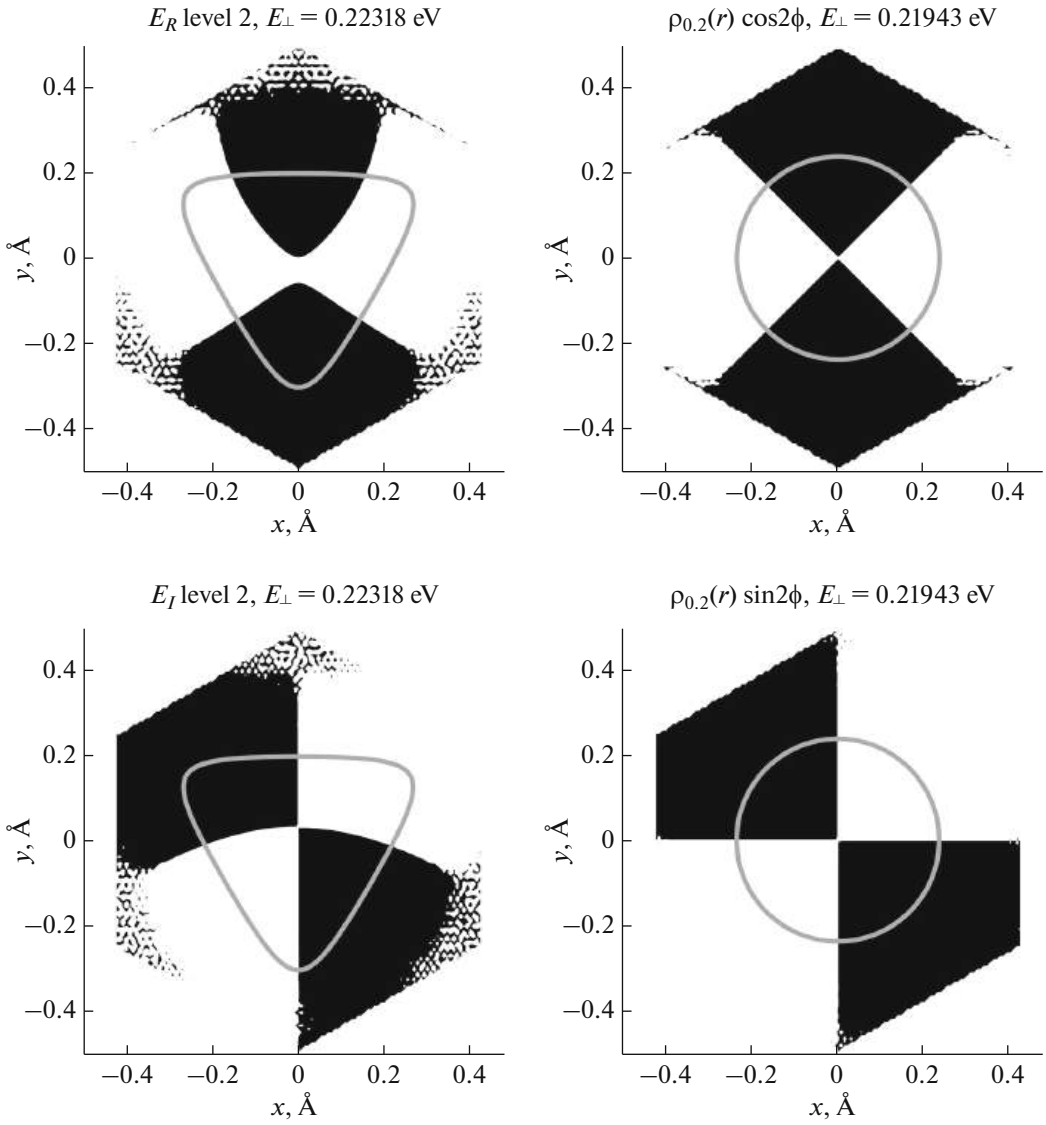

Fig. 4. Same as Fig. 3, for states with $E_\perp = 0.22318$ eV in a potential well (1) and for states with $E_\perp = 0.21943$ eV in a potential well (8).

lated numerically. From quasi-classical arguments (e.g., [1]), it follows that the number of bound states in the well increases with increasing $E_\parallel$. It turns out that for an energy of 5 GeV, bound states of the symmetry type A_2 are still absent, while at an energy of 6 GeV, the first such state appears near the upper edge of the potential well (its depth is 0.3278 eV). Such behavior is not surprising, since the symmetry of the wave functions of this type suggests the presence of at least three nodal lines in the azimuthal direction, which corresponds to a relatively high average kinetic energy of the state. The graphs of all the wave functions for the bound stationary states at $E_\parallel = 6$ GeV are shown in Fig. 2, along with the energy level diagram for the transverse motion $E_\perp$.

It is interesting to compare the wave functions of stationary states in the potential well (1) with similar wave functions in an axially symmetric potential well. For this comparison, a potential well in the form of a power function was taken,

$$U(x,y) = \gamma r^\delta, \quad r = \sqrt{x^2 + y^2}, \tag{8}$$

where the coefficients γ and δ were selected such that the phase space available for motion with an energy less than or equal to the given value $E_\perp$ was adjusted accordingly, i.e.,

$$\int\limits_{H(x,y,p_x,p_y)\le E_\perp} dxdydp_xdp_y \tag{9}$$

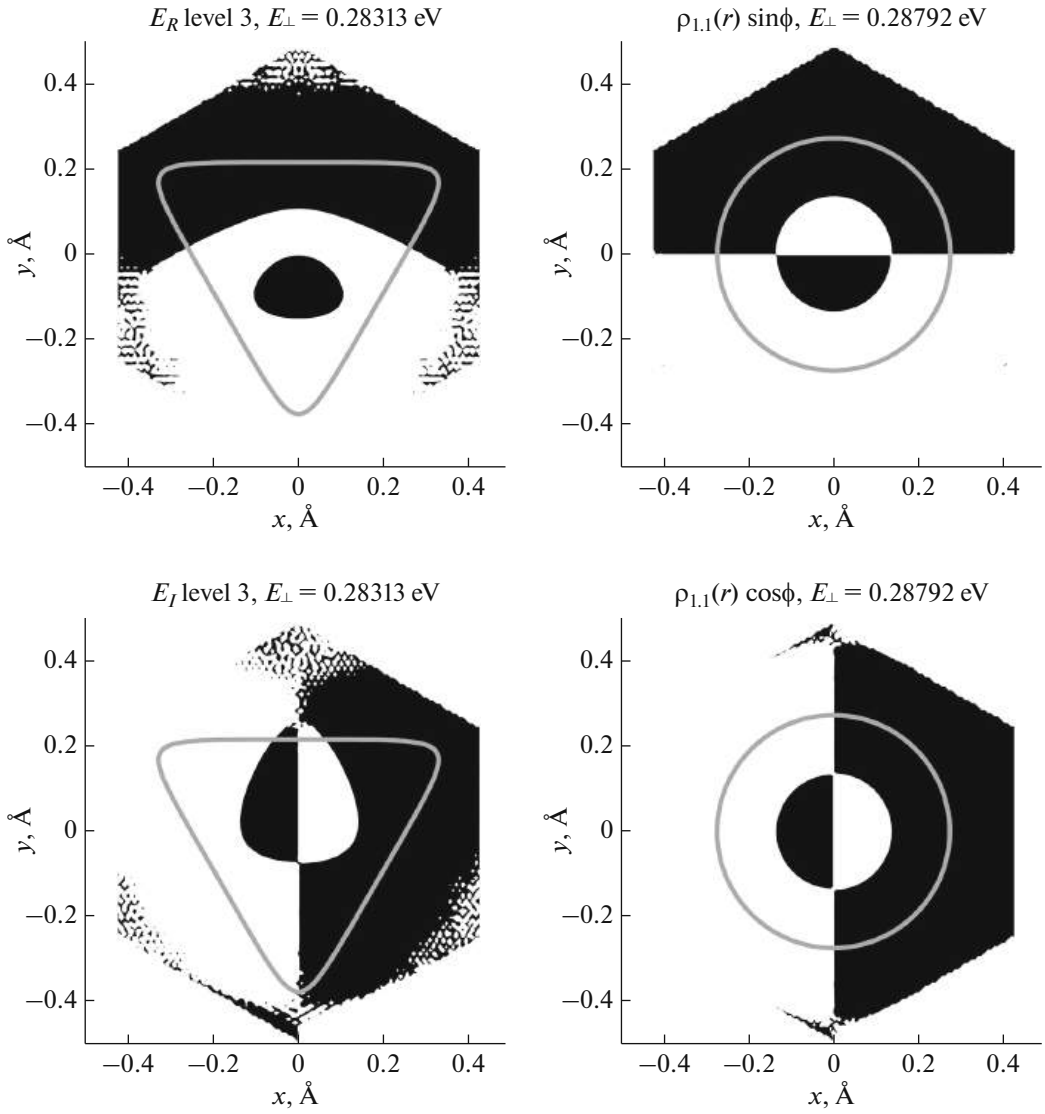

Fig. 5. Same as Fig. 3, for states with $E_\perp = 0.28313$ eV in a potential well (1) and for states with $E_\perp = 0.28792$ eV in a potential well (8).

(where $H(x, y, p_x, p_y)$ is the classical Hamiltonian of the system) was the same for both potentials (1) and (8). For positrons with the energy $E_\parallel = 6$ GeV, this selection of coefficients resulted in $\gamma = 3.1807$ and $\delta = 1.85$, provided that the distance to the axis of the potential well is expressed in Angstroms in Eq. (8), and the potential energy is given in electron volts.

In the field of an axially symmetric potential, along with the transverse energy $E_\perp$, the projection of the particle's orbital angular momentum m onto the axis of the potential well is retained. The presence of these two integrals of motion makes the two-dimensional system integrable. Stationary states in this case are characterized by two quantum numbers: the radial quantum number n_r (corresponding to the number of zeros of the radial part of the wave function, excluding the zeros at $r = 0$ and $r \to \infty$) and the orbital quantum number m (for example, problem 4.7 in [26], as well as [7–9]). States with $m = 0$ are nondegenerate, while states with $m \neq 0$ are doubly degenerate with respect to the sign of m (i.e., with respect to the direction of the projection of the particle's orbital angular momentum onto the axis of the potential well). In the latter case, a pair of wave functions corresponding to such a doubly degenerate energy level is conveniently chosen to be purely real in the form of

$$\rho_{n_r,|m|}(r)\sin|m|\phi, \quad \rho_{n_r,|m|}(r)\cos|m|\phi. \tag{10}$$

The values of these quantum numbers for a specific state can be determined by counting the nodal lines on the wave-function graph. For convenience in this counting, regions where the function takes positive values are shaded white, and regions with negative values are shaded black, as shown in Figs. 3–6. The right columns of these figures provide examples of wave

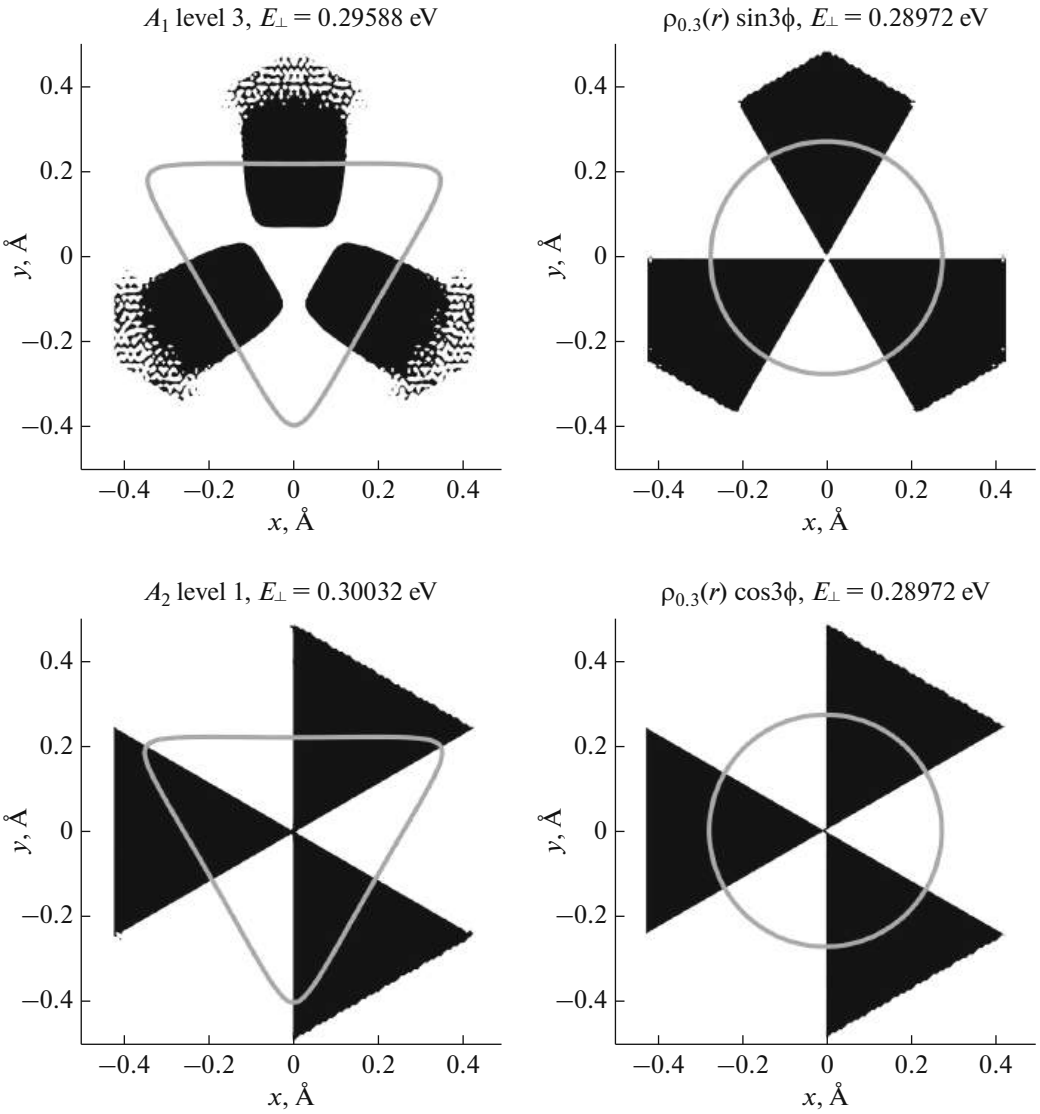

Fig. 6. Same as Fig. 3, for states with $E_\perp = 0.29588$ eV and $E_\perp = 0.30032$ eV in a potential well (1) and for states with $E_\perp = 0.28972$ eV in a potential well (8).

functions of the form (10) for stationary states in the potential well (8).

Group theory predicts (e.g. , [27]) that the perturbation of the field of an axially symmetric potential with C_{3v} symmetry (as in the case of potential (1)) leads to elimination of the degeneracy of states with $|m|$ being a multiple of three, while the degeneracy is retained in other cases. Comparison of the wave functions of potential (1) with those of the axially symmetric potential (8) illustrates this conclusion: the pair of degenerate states with $n_r = 0$, $|m| = 1$ under the influence of perturbation transforms into a pair of similarly degenerate lowest states, corresponding to the symmetry type E (Fig. 3), the pair of states with $n_r = 0$, $|m| = 2$ transforms into a second pair of E-type states (Fig. 4), and the pair of states with $n_r = 1$, $|m| = 1$ transforms into a third pair of E-type states (Fig. 5). In contrast, the pair of states with $n_r = 0$, $|m| = 3$ splits under the action of the perturbation into two nondegenerate states: the third A_1-type state and the first (and only for $E_\parallel = 6$ GeV) A_2-type state (Fig. 6).

The nodal lines of the wave functions in Figs. 3–6 allow us to trace the relationship between the states in the potentials (8) and (1). Additionally, the character of the nodal lines in the wave functions of the potential (1) reveals a significant difference from the integrable potential (8). As shown by the study using Poincaré sections [2, 28], in the upper part of potential (1), the second integral of motion is absent for the overwhelming majority of initial conditions, which makes the equation of motion in potential (1) nonintegrable (unlike the axially symmetric potential (8)), and the

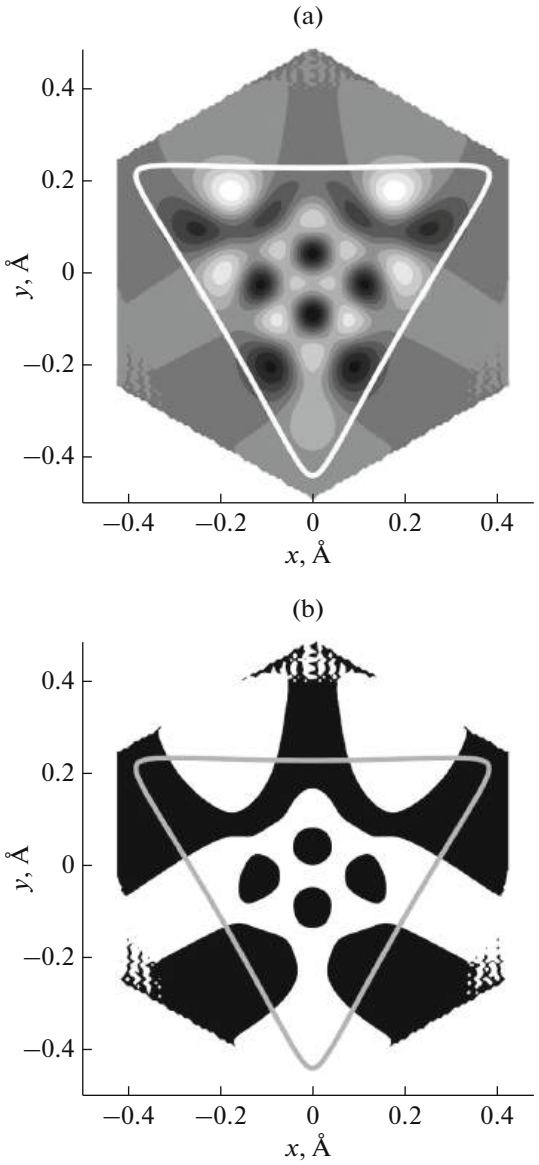

Fig. 7. (a) Wave function of an E_R-type state for a positron with energy $E_\parallel = 20$ GeV in a potential well (1), corresponding to $E_\perp = 0.31807$ eV, and (b) the graph of the same wave function, where regions of positive values are shaded in white and regions of negative values are shaded in black.

motion itself chaotic. One manifestation of dynamical chaos in quantum mechanics is the specific pattern of nodal lines of the wave function: in the regular (integrable) case, these lines intersect, forming a chessboard-like pattern, while in the nonintegrable (chaotic) case, they avoid intersections [8, 9, 17, 19]. Examples of this avoidance are visible in the top-left graphs of Figs. 4–6.

Indeed, this feature, along with other characteristic aspects of quantum chaos, is most prominent in the quasi-classical region of parameter values, where the density of energy levels is high and many nodes and antinodes of the wave function fit within the potential well. Figure 7 presents an example of the wave function of a stationary state of a positron with the energy $E_\parallel = 20$ GeV in the upper part of the potential well (1). As expected for a chaotic, nonintegrable system, we observe the typical absence of intersections of the nodal lines, which is a hallmark of chaotic quantum behavior.

CONCLUSIONS

In this work, positron channeling near the [111] direction of a silicon crystal with energies of 5, 6, and 20 GeV has been considered. Using a previously developed algorithm, all energy levels of the transverse motion and their corresponding eigenfunctions have been numerically calculated. Graphs of all wave functions for positrons with an energy of 6 GeV are presented in this work, while complete sets of wave-function graphs for the 5 and 20 GeV cases are also published in [29].

The wave functions found have been classified according to the irreducible representations of the group C_{3v}. This group describes the symmetry of the potential well in which the transverse motion of channeling positrons occurs. The work demonstrates how a perturbation, which possesses the symmetry of an equilateral triangle, leads to differences between these wave functions and the wave functions in an axially symmetric potential well. In the upper part of the potential well, where the classical motion of the particle is nonintegrable for the majority of initial conditions, qualitative features appear in the structure of the wave functions, distinguishing them from the wave functions of integrable systems. Such differences are most noticeable for positrons with an energy of 20 GeV, as the increased density of energy levels makes the quasi-classical approximation valid, in which quantum chaos effects are manifested.

FUNDING

This work was supported by ongoing institutional funding. No additional grants to carry out or direct this particular research were obtained.

CONFLICT OF INTEREST

The authors of this work declare that they have no conflicts of interest.

REFERENCES

1. A. I. Akhiezer and N. F. Shul'ga, *High Energy Electrodynamics in Matter* (Nauka, Moscow, 1993) [in Russian].
2. A. I. Akhiezer, N. F. Shul'ga, V. I. Truten', A. A. Grinenko, and V. V. Syshchenko, Usp. Fiz. Nauk **165** (10), 1165

(1995).
https://doi.org/10.3367/UFNr.0165.199510c.1165

3. D. S. Gemmel, Rev. Mod. Phys. **46**, 129 (1974).
https://doi.org/10.1103/RevModPhys.46.129

4. U. I. Uggerhøj, Rev. Mod. Phys. **77**, 1131 (2005).
https://doi.org/10.1103/RevModPhys.77.1131

5. J. Lindhard, Kongel. Dan. Vidensk. Selsk., Mat.-Fys. Medd. **34** (14), 1 (1965).

6. N. F. Shul'ga, V. V. Syshchenko, A. I. Tarnovsky, and A. Yu. Isupov, J. Surf. Invest.: X-ray, Synchrotron Neutron Tech. **9**, 721 (2015).
https://doi.org/10.1134/S1027451015040199

7. N. F. Shul'ga, V. V. Syshchenko, A. I. Tarnovsky, and A. Yu. Isupov, Nucl. Instrum. Methods Phys. Res., Sect. B **370**, 1 (2016).
https://doi.org/10.1016/j.nimb.2015.12.040

8. N. F. Shul'ga, V. V. Syshchenko, A. I. Tarnovsky, and A. Yu. Isupov, J. Phys.: Conf. Ser. **732**, 012028 (2016).
https://doi.org/10.1088/1742-6596/732/1/012028

9. N. F. Shul'ga, V. V. Syshchenko, A. I. Tarnovsky, and A. Yu. Isupov, J. Surf. Invest.: X-ray, Synchrotron Neutron Tech. **10**, 458 (2016).
https://doi.org/10.1134/S102745101602035X

10. V. V. Syshchenko and A. I. Tarnovsky, J. Surf. Invest.: X-ray, Synchrotron Neutron Tech. 15, 728 (2021).
https://doi.org/10.1134/S1027451021040200

11. V. V. Syshchenko, A. I. Tarnovsky, A. Yu. Isupov, and I. I. Solovyev, J. Surf. Invest.: X-ray, Synchrotron Neutron Tech. **14**, 306 (2020).
https://doi.org/10.1134/S1027451020020354

12. N. F. Shul'ga, V. V. Syshchenko, A. I. Tarnovsky, V. I. Dronik, and A. Yu. Isupov, J. Instrum. **14**, C12022 (2019).
https://doi.org/10.1088/1748-0221/14/12/C12022

13. V. V. Syshchenko, A. I. Tarnovsky, V. I. Dronik, and A. Yu. Isupov, J. Surf. Invest.: X-ray, Synchrotron Neutron Tech. **15**, 73 (2022).
https://doi.org/10.1134/S1027451022020203

14. V. V. Syshchenko, A. I. Tarnovsky, V. I. Dronik, and A. Yu. Isupov, J. Surf. Invest.: X-ray, Synchrotron Neutron Tech. **17**, 7007 (2023).
https://doi.org/10.1134/S1027451023030321

15. L. D. Landau and E. M. Lifshits, *Course of Theoretical Physics, Vol. 3: Quantum Mechanics: Non-Relativistic Theory* (Pergamon Press, Oxford, 1977); Fizmatlit, Moscow, 2016).

16. M. C. Gutzwiller, *Chaos in Classical and Quantum Mechanics* (Springer-Verlag, 1990).
https://doi.org/10.1007/978-1-4612-0983-6

17. H.-J. Stöckmann, Quantum Chaos: An Introduction (Cambridge Univ. Press, Cambridge, 2000; Fizmatlit, Moscow, 2004).

18. L. E. Reichl, The Transition to Chaos: Conservative Classical Systems and Quantum Manifestations, 2nd ed. (Springer, New York, 2004; RKhD, Moscow–Izhevsk, 2008).

19. Y. Bolotin, A. Tur, and V. Yanovsky, *Chaos: Concepts, Control and Constructive Use* (Springer Int., Switzerland, 2017).
https://doi.org/10.1007/978-3-319-42496-5

20. M. Hénon and C. Heiles, Astronom. J. **69**, 73 (1964).
https://doi.org/10.1086/109234

21. M. J. Davis and E. J. Heller, J. Chem. Phys. **75**, 246 (1981).
https://doi.org/10.1063/1.441832

22. V. V. Syshchenko, A. I. Tarnovsky, A. S. Parakhin, and A. Yu. Isupov, J. Surf. Invest.: X-ray, Synchrotron Neutron Tech. **18** (2), 274 (2024).
https://doi.org/10.1134/S1027451024020186

23. M. D. Feit, J. A. Fleck, and Jr., A. Steiger, J. Comput. Phys. **47**, 412 (1982).
https://doi.org/10.1016/0021-9991(82)90091-2

24. Shul'ga, N.F., V. V. Syshchenko, and V. S. Neryabova, J. Surf. Invest.: X-ray, Synchrotron Neutron Tech. **7**, 279 (2013).
https://doi.org/10.1134/S1027451013020183

25. N. F. Shul'ga, V. V. Syshchenko, and V. S. Neryabova, Nucl. Instrum. Methods Phys. Res., Sect. B **309**, 153 (2013).
https://doi.org/10.1016/j.nimb.2013.01.022

26. V. M. Galitskii, B. M. Karnakov, and V. I. Kogan, *Problems in Quantum Mechanics* (Nauka, Moscow, 1981) [in Russian].

27. D. A. Shapiro, *Group Representations and their Applications in Physics* (Novosib. Gos. Univ., Novosibirsk, 2005) [in Russian].

28. A. Yu. Isupov, V. V. Syshchenko, and A. S. Parakhin, Prikl. Matem. Fiz. **55** (1), 49 (2023).
https://doi.org/10.52575/2687-0959-2023-55-1-49-56

29. A. Yu. Isupov, V. V. Syshchenko, A. I. Tarnovsky, and A. S. Parakhin, Prikl. Matem. Fiz. 56 (4), 320 (2024).
https://doi.org/10.52575/2687-0959-2024-56-4-320-327

Translated by O. Zhukova